Quantification of the Anatomical Remodelling of the Ventricles of ARVC Patients, an MRI Based Study

Peter Marinov[1], Ernesto Zacur[2], Michele Orini[3], Pier D Lambiase[3], Vincente Grau[2], Blanca Rodriguez[1], Alfonso Bueno-Orovio[1]

[1]Department of Computer Science, University of Oxford, Oxford, UK
[2]Institute of Biomedical Engineering, Department of Engineering Science, University of Oxford, Oxford, UK
[3]Department of Cardiac Electrophysiology, The Barts Heart Center, St. Bartholomew's Hospital, London, UK

Abstract

Arrhythmogenic Right Ventricular Cardiomyopathy (ARVC) is a potentially lethal form of cardiomyopathy, with a high incidence of mortality amongst the young and in competitive athletes. It is characterized by fibrofatty replacement of the ventricular myocardium with negative impact on RV function. No ARVC specific treatments exist to date, although the pathophysiology is related to mutations in desmosomal adhesion proteins with downstream effects on cellular differentiation, communication, electrophysiology and survival. To this purpose, we seek to quantify the extent of anatomical remodelling in four early stage ARVC human patients. The right ventricular end diastolic volume is significantly increased (+44%) with respect to a control group. The ventricular muscle volume, comprising of the left ventricle, right ventricle and septum is drastically higher (+79%) than in our control group. These findings suggest a need to better understand the role of anatomical deformations in ARVC disease progression. Furthermore, this is a validation of a novel, semi-automatic imaging pipeline, which can be adopted in larger human studies.

1. Introduction

ARVC typically manifests itself in the right ventricle first, before progressing to the left ventricle. The 2010 Revised Task Force criteria [1] for diagnosis of ARVC include the assessment of the performance and integrity of the right ventricle. Some studies point to dilation of the right ventricle as a common phenotype in desmosome mutated ARVC mice [2] and in patients [3], in which right ventricular ejection fraction is significantly compromised. To date, no magnetic resonance imaging (MRI) based quantification of the degree of dilation of the right ventricle has been performed on an ARVC cohort, although similar studies using 3D echocardiography have been performed [4]. Accurate MRI measurement of right ventricular (RV) volume in ARVC patients could improve diagnosis and help clinicians track the progress of the disease. In this work, we measure the volume of the ventricular ARVC chambers and muscle mass, using an in house algorithm. The algorithm takes as inputs a standard cardiac MRI acquisition, as well manual segmentations of the endocardial and epicardial borders and creates a fine, ventricular, patient-specific mesh. Geometric analysis on the patient meshes allows for a volumetric and muscle volume quantification of unprecedented accuracy.

2. Methods

2.1. MRI to Ventricular Mesh Algorithm

Recently, we presented an algorithm able to create a surface ventricular mesh from sparse, heterogeneous, non-parallel, cross-sectional, non-coincidental contours and showed the algorithm is able to reconstruct ventricular surfaces from MRI data [5]. Our approach uses a composition of smooth approximations towards the maximization of the data fitting, ensuring a good matching to the input data as well as optimal interpolation characteristics. The pipeline can choose between degree of data fitting and smoothness of the final meshes. The results presented in this study are produced following the pipeline, described in Fig.1, and are obtained using a set up emphasising smoothness. For the patients and controls analysed, the mean contour to mesh discrepancy is under 1.7mm for the left ventricular (LV) epicardium and falls below 2.5mm for the RV endocardium. Since we are

studying global ventricular measures, such as chamber volume and muscle mass, the results will not change significantly for meshes that are more rigorously fit to the data points.

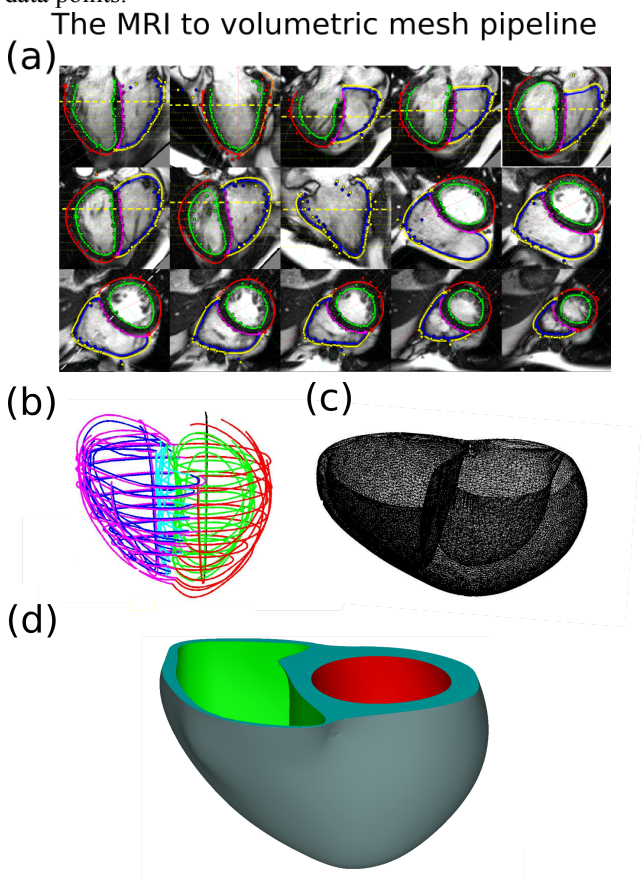

Figure 1. The MRI to personalised ventricular mesh pipeline. (a) The DICOMs are contoured manually, defining the left endocardial wall (green), left epicardial wall (red) and right endocardial wall (blue). (b) The contours are aligned to correct for respiratory movement of the patient and contouring inaccuracies and the septum is resolved. (c) A coarse triangular surface mesh of the ventricles is generated by fitting to the contours. (d) The surface mesh is filled with tetrahedra from (c) and refined to an edge length of 4mm. In order to facilitate the volumetric calculation, the mesh is closed with a flat surface lid, covering the whole basal area of the ventricles.

2.2. Computing Triangular Element Volumes

The surface area of the ventricles is computed by summing up the areas of the constituent mesh triangles. We use the so called centroid area normal algorithm, first coined by Hughes et al. 1996 [6]. By computing the vectors connecting the edges of a given triangle we can quickly find its area as shown in Fig.2.

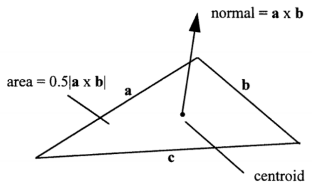

Figure 2. The area of a triangle using cross products.

The intra-cavital volume is computed using an adaptation of Gauss' theorem:

$$V = \int\int\int_{V} (\nabla . \mathbf{F})\, dV = \oiint (\mathbf{F}.\mathbf{n}) dS \qquad (1)$$

where **F** is a vector field, **n** is the normal vector to an infinitesimal surface area element dS, and dV is an infinitesimal volume element. In order to compute the volume of an element, we look for a vector field **F** satisfying $\nabla . \mathbf{F} = 1$. The form of **F** is not unique, for instance $\mathbf{F} = (x,0,0)^T$ or $\mathbf{F} = (x,y,z)^T/3$ are both valid choices, and yet we choose the latter since it is symmetrical.

When considering closed triangular meshes, the right hand side of Equation (1) can be manipulated to follows

$$\int_{\partial V} (\mathbf{F}.\mathbf{n}) dS = \sum_i \int_{Ti} (\mathbf{F}.\mathbf{n}_i) dS \qquad (2)$$

where we are summing over all triangles composing the surface. For each triangle T_i, the normal $\mathbf{n}_i$ is unique and the integral can be computed analytically using

$$\int_{Ti} (\mathbf{F}.\mathbf{n}_i) dS = A_i \, (\mathbf{c}_i.\mathbf{n}_i \,)/3 \qquad (3)$$

where c_i are the coordinates of the centroid of the i^{th} triangular element in our mesh and A_i is the corresponding triangle area, as illustrated in Fig.2. A requirement of the volume calculation is that all of the normals of the triangles point outwards of the object whose volume we are computing and that the surface is watertight. Interestingly, this is a the first moment of the surface, higher order moments can be calculated [7].

2.3. Uncertainty of Measurement

There are two major potential sources of uncertainty in this study. The first is the uncertainty in the manual contouring process. In order to minimise this uncertainty, the same person contoured all of the patient MRIs in a short space of time. In this way, if there is any bias of measurement, it is present for all the patients studied in the ARVC cohort. The set of control patients was contoured by a specialist cardiologist, meaning a systematic bias could be present in contouring style amongst the 2 groups.

The second source of uncertainty is the one introduced in the process of creating surfaces from a set of contours. The local uncertainty, defined as the maximum distance between a contour and its nearest surface area element is in the order of a few millimeters. This mismatch is illustrated in Fig.3 for ARVC patient 1 and arises whenever there is discrepancy between the contours of 2 intersecting frames. The discrepancy is minimised by the surface generating algorithm, which makes a compromise between contrasting contours, choosing the middle ground.

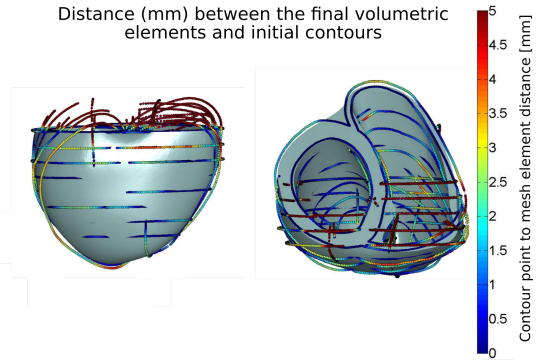

Figure 3. The volumetric mesh and initial contours are shown for ARVC patient 1. The colour on the contours is an indication of distance to the nearest element in the mesh. None of the contours lie more than 5mm away from the final mesh.

2.4. Patient Cohort

The patients are all previously diagnosed with early to intermediate stage ARVC. Patient 1 has a mutation in the gene responsible for making plakophilin 2, patients 2 and 3 have a mutation in a corresponding desmoplakin gene, whilst patient 4 has no known gene mutation. All of the patients are male, with mean age 58±4 years. Three out of four patients have RV dilation, as reported by a cardiologist. The imaging acquisition protocol, as well as the patients studied, are described in detail in a previous publication [8].

3. Results

The digital ARVC ventricles are first scrutinised for any apparent physiological deformations. By naked eye, patients 1 and 2 are clearly found to have RV enlargement and all patients in the ARVC group had a thick free left ventricular wall. The raw ventricular meshes are presented in Fig.4.

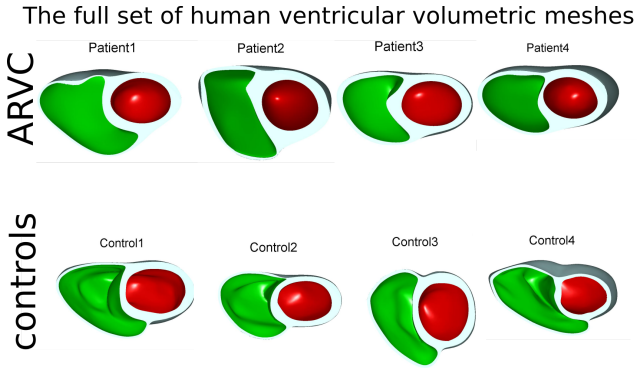

Figure 4. The ARVC (above) and control (below) patient group ventricular meshes are shown. In red is depicted the left ventricle and in green the right ventricle.

Our quantitative analysis finds a drastic enlargement in RV end diastolic volume. Mean RV chamber volume for the ARVC cohort is $1.85 \pm 0.51 \text{x} 10^{5}\ mm^{3}$ versus $1.28 \pm 0.47 \text{x} 10^{5}\ mm^{3}$ for the control cohort, a 44% increase. The RV chamber volumes are plotted in Fig.5b. On the other hand, mean LV chamber volume is similar between the 2 groups, $1.44 \pm 0.13 \text{x} 10^{5}\ mm^{3}$ for the ARVC cohort versus $1.31 \pm 0.48 \text{x} 10^{5}\ mm^{3}$ for the control population, as can be seen in Fig.5a.

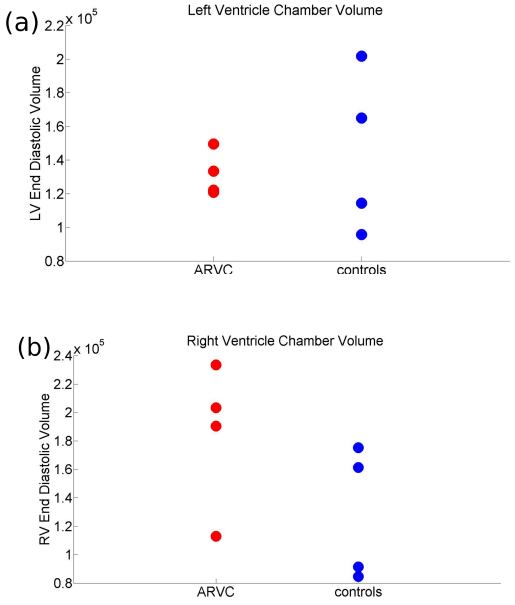

Figure 5. Left (a) and right (b) ventricular chamber volumes are plotted. Despite having a slightly smaller mean left ventricular chamber volume, the ARVC patients have a 44% larger mean right ventricular chamber volume.

The ratio of RV to LV chamber end diastolic volumes is above 1 for all of the ARVC patients studied, as the mesh analysis in Fig.6 shows. This means the right ventricle has a significantly larger chamber volume than its left counterpart, in agreement with literature [9]. Interestingly, the RV to LV volumes ratio is higher for every patient in the ARVC cohort than the maximum in the control group. More specifically, the ARVC cohort mean volumes ratio is 1.41 and 0.88 for the control group.

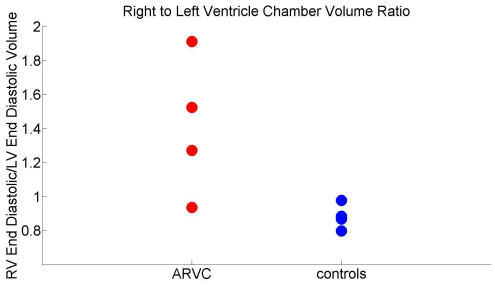

Figure 6. The ratio of right ventricular to left ventricular chamber volumes is plotted in red for the ARVC cohort and blue for the control cohort. The dimensionless quantity is consistently higher amongst ARVC sufferers in this cohort.

We further find an enlargement in the total ventricular muscle volume of the ARVC cohort, as reported in Fig.7. The mean ventricular muscle volume of the ARVC cohort is $2.2\pm0.64\times10^{5}\ mm^{3}$ and the control population mean is $1.23\pm0.41\times10^{5}\ mm^{3}$, suggesting a 78.9% dilation of muscle volume amongst cohorts.

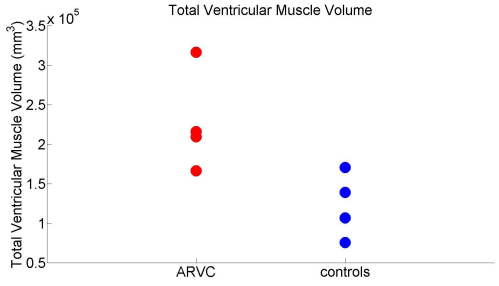

Figure 7. The total ventricular myocardial volume is plotted in red for the ARVC cohort and blue for the control cohort. Muscle volume is found to be consistently higher amongst ARVC sufferers in this cohort.

4. Conclusions

A 3D analysis involving a geometric reconstruction of the human ventricular anatomy of a cohort of 4 ARVC patients has been performed from MRI data. Digital representations of the geometries of the patient ventricles have been created for this and a control cohort. Using an adaptation of Gauss' theorem, the chamber volumes of each patient ventricle as well as the myocardial muscle volumes were calculated. The RV mean ventricular chamber volume of the control group is in excellent agreement with a recent, large scale study that used computed tomography angiography to compute ventricular chamber volumes [9]. A comparison between the ARVC and control cohorts revealed a 44% increase in the mean right ventricular chamber volume of ARVC sufferers and a 79% increase in the volume of the constituent muscle mass. It is worth noting that left ventricular chamber volumes were of similar size among the two groups. These results highlight the extent of the anatomical remodelling present in ARVC and the right ventricular nature of the remodelling.

The calculations need to be repeated in a study of a larger patient group in order to acquire statistical significance. The muscle mass of each ventricle individually was not computed. It would be of interest to explore if chamber dilation and ventricular wall thickness follow a similar pattern. Another possible avenue of research is the impact of this altered ventricular anatomy on the 12-lead ECG, an avenue to be addressed using whole ventricular bidomain based simulations.

Acknowledgments

This work was funded by a PhD scholarship from the UK Engineering and Physical Sciences Research Council (PM), a Wellcome Trust Senior Research Fellowship in Basic Biomedical Sciences (BR, EZ), a BHF Intermediate Basic Science Research Fellowship (AB), UCLH Biomedicine NIHR (PL), a BHF grant (MO), an MRC grant (MO,PL) and an NC3Rs Infra-structure for Impact Award (BR, AB).

Address for correspondence:
Peter Marinov, Wolfson Building, Parks Rd, Oxford OX1 3QD
peter.marinov@cs.ox.ac.uk

References

[1] Marcus, McKenna, Sherrill, *et al. Eur Hear J* 2010;31.

[2] Kant, Krull, Eisner, *et al. Cell Tissue Res* 2012;**348**:249–59.

[3] Gemayel, Pelliccia, Thompson. *J Am Coll Cardiol* 2001;**38**:1773–81.

[4] Kjaergaard, Hastrup Svendsen, Sogaard, *et al. J Am Soc Echocardiogr* 2007;**20**:27–35.

[5] Villard, Carapella, Ariga, *et al. Springer*, Cham 2017. 169–81.

[6] Hughes, D'Arcy, Maxwell, *et al. Phys Med Biol* 1996;**41**:1809–21.

[7] Millan, Dempere-Marco, Pozo, *et al. IEEE Trans Med*

Imaging 2007;**26**:1270–82.
[8] Andrews, Srinivasan, Rosmini, *et al. Circ Arrhythmia Electrophysiol* 2017;**10**.
[9] Fuchs, Mejdahl, Kühl, *et al. Eur Hear J – Cardiovasc Imaging* 2016;**17**:1009–17.